

Volatile dilution during magma injections and implications for volcano explosivity

Mike Cassidy^{1*}, Jonathan M. Castro¹, Christoph Helo¹, Valentin R. Troll², Frances M. Deegan², Duncan Muir², David A. Neave³, and Sebastian P. Mueller¹

¹Institute of Geosciences, University of Mainz, D-55122 Mainz, Germany

²Centre for Experimental Mineralogy, Petrology and Geochemistry, Department of Earth Sciences, Uppsala University, 1477 Uppsala Sweden

³Institute of Mineralogy, Leibniz University of Hannover, 30167 Hannover, Germany

ABSTRACT

Magma reservoirs underneath volcanoes grow through episodic emplacement of magma batches. These pulsed magma injections can substantially alter the physical state of the resident magma by changing its temperature, pressure, composition, and volatile content. Here we examine plagioclase phenocrysts in pumice from the 2014 Plinian eruption of Kelud (Indonesia) that record the progressive capture of small melt inclusions within concentric growth zones during crystallization inside a magma reservoir. High-spatial-resolution Raman spectroscopic measurements reveal the concentration of dissolved H₂O within the melt inclusions, and provide insights into melt-volatile behavior at the single crystal scale. H₂O contents within melt inclusions range from ~0.45 to 2.27 wt% and do not correlate with melt inclusion size or distance from the crystal rim, suggesting that minimal H₂O was lost via diffusion. Instead, inclusion H₂O contents vary systematically with anorthite content of the host plagioclase ($R^2 = 0.51$), whereby high anorthite content zones are associated with low H₂O contents and vice versa. This relationship suggests that injections of hot and H₂O-poor magma can increase the reservoir temperature, leading to the dilution of melt H₂O contents. In addition to recording hot and H₂O-poor conditions after these injections, plagioclase crystals also record relatively cold and H₂O-rich conditions such as prior to the explosive 2014 eruption. In this case, the elevated H₂O content and increased viscosity may have contributed to the high explosivity of the eruption. The point at which an eruption occurs within such repeating hot and cool cycles may therefore have important implications for explaining alternating eruptive styles.

INTRODUCTION

The repeated supply of new magma into crystallizing magmatic reservoirs is considered to be a necessary process during magma reservoir growth (Menand et al., 2015). However, the time periods between incremental recharge growth can be large, leading to cooling and crystallization, which can limit the mobility and therefore eruptibility of magmas (Cooper and Kent, 2014). In order to provide the necessary thermochemical conditions for an eruption injections of hot magma are required to increase the proportion of melt relative to crystals (Burgisser and Bergantz, 2011). Such pulsatory recharges are ubiquitous in nature, yet little quantitative information exists about how they can affect the temperature, crystallinity, and volatile budget of the resident magma prior to eruption, all of which can have implications for eruptive style. Magma mixing is a natural consequence of recharge and is thought to have contrasting effects on the explosivity of an eruption. Some

studies suggest that mixing can initiate explosive volcanism by increasing magma overpressure through the influx of magma and excess volatiles to the system (Sparks et al., 1977). In contrast, recent case studies have shown that magma mixing may decrease explosive potential by causing heat-driven viscosity and H₂O-solubility changes, leading to volatile exsolution and pre-eruptive outgassing (Ruprecht and Bachmann, 2010). It is thus imperative to quantify how intensive parameters, such as temperature and volatile contents, change during magma mixing cycles.

Although techniques such as Fourier transform infrared spectroscopy (FTIR), secondary ion mass spectrometry (SIMS), and Raman spectroscopy can be used to measure the H₂O content of volcanic glasses, groundmass (or matrix) glasses normally degas during ascent and eruption and thus often fail to record primary H₂O content. Therefore, *in situ* measurement of melt inclusions trapped during magma storage provides one of the best direct ways of gaining information about pre-eruptive magmatic H₂O contents (Wallace, 2005). However, accurate

measurement of H₂O contents in melt inclusions can be compromised by problems such as vapor leakage from ruptured inclusions, boundary layer processes, postentrapment modification, diffusive transfer, and late entrapment (where channels connecting melt inclusions are only closed off to the matrix melt at a late stage; e.g., Kent, 2008, Baker, 2008; Gaetani et al., 2012, Humphreys et al., 2008). Some of these problems can be avoided by studying rapidly quenched samples (Lloyd et al., 2013), or by restricting analysis to small, pristine melt inclusions that are less susceptible to volatile loss through melt inclusion rupture (Kent, 2008). Raman spectroscopy is an emerging nondestructive technique in geosciences (e.g., Behrens et al., 2006) that offers high spatial resolution (1–2 μm²) and relatively easy sample preparation, and thus has advantages over other *in situ* methods such as FTIR and SIMS. For these reasons we use Raman spectroscopy to measure the H₂O contents of melt inclusions within individual plagioclase phenocrysts that erupted in the explosive Plinian event at Kelud volcano, Indonesia, in A.D. 2014.

GEOLOGIC SETTING

Kelud volcano is located in the Java segment of the Sunda Arc and is highly active, having erupted eight times since A.D. 1900 (Siebert and Simkin, 2002). Erupted bulk material at Kelud is consistently basaltic andesite in composition, despite the volcano having highly contrasting eruptive styles that vary from dome-forming effusive eruptions in 1920 and 2007, to Plinian eruptions in 1990 and 2014 (e.g., Jeffery et al., 2013; this study). The samples used in this study are from the 2014 Plinian eruption, which showed only a few weeks of increased unrest prior to the eruption (Caudron et al., 2015). The 2014 event, despite erupting relatively small volumes and lasting only a few hours, had an estimated intensity between that of Mount St. Helens (Washington State, USA) and Pinatubo (Philippines) (Caudron et al., 2015); the first stages were associated with an eruption column 26 km in height (Kristiansen et al., 2015).

*E-mail: mcassidy@uni-mainz.de

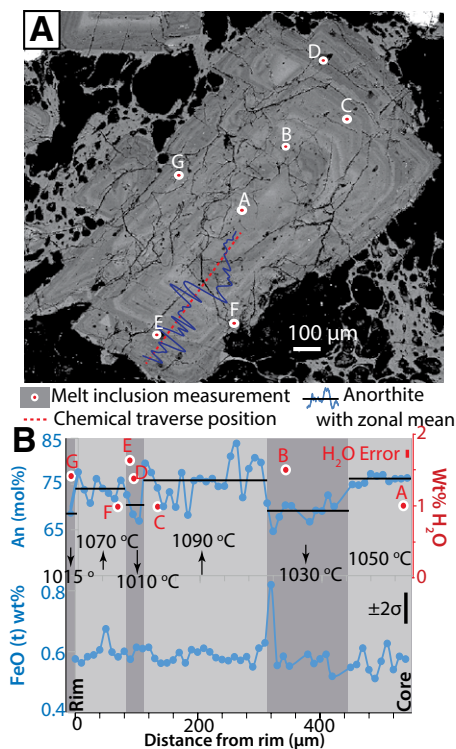


Figure 1. A: Backscattered electron (BSE) image of a concentrically zoned plagioclase with melt inclusion H₂O measurement points (via Raman spectroscopy) and chemical traverse line highlighted. Where inclusions were situated away from the chemical profile, calibrated grayscale anorthite values were used. B: Molar anorthite and total (t) iron oxide profiles plotted with corresponding H₂O measurements of the melt inclusions located in their respective high and low anorthite content zones (light and dark gray bands, respectively, from BSE image). Temperatures were calculated after Waters and Lange (2015).

METHODS

Pumice lapilli samples were collected from the crater edge shortly after the 2014 eruption. Three samples were washed, cut, impregnated in epoxy resin, and then made into polished thin sections and wafers for Raman studies and electron probe microanalyses (EPMA). EPMA, FTIR, and Raman spectroscopy were conducted at the Institute of Geosciences at the University of Mainz, Germany (see the GSA Data Repository¹). For Raman analysis, a blue laser (488 nm) and 50× magnification were used with a dwell time of 25 s and 40 repetition cycles to ensure high-resolution spectra by improving the signal-to-noise ratio. Backscattered Raman radiation was collected over a large range of 50–4000 cm⁻¹ using a 300 l/mm grating, confocal hole of 400 μm, slit of 100 μm, and a laser power of 1 mW at the sample. Spectra intensities were corrected for

¹GSA Data Repository item 2016345, Figures DR1–DR9 and Tables DR1–DR5, is available online at <http://www.geosociety.org/pubs/ft2016.htm> or on request from editing@geosociety.org.

frequency dependence according to Long (1977), before baselines were fitted by selecting points either side of the silicate network (~100–1300 cm⁻¹) and H₂O peaks (~3000–3800 cm⁻¹). The spectra were subsequently normalized to the integrated area of the silicate network bands and then the H₂O peak was integrated. These integrated areas were converted to H₂O contents using a calibration curve from known internal standards of similar glass compositions measured with FTIR (Fig. DR1 in the Data Repository). Incorporating processing, Raman analyses have a 1σ precision of 0.22 wt% H₂O (Table DR1).

RESULTS AND DISCUSSION

Kelud 2014 pumices have basaltic andesite compositions, are phenocryst rich (53%–75%; mean of 59%), and contain a mineral assemblage of plagioclase, orthopyroxene, clinopyroxene, and magnetite. Plagioclase crystals have the following zoning types and abundances: concentric (63%), simple normal (21%), patchy (9%), and unzoned (7%) (Fig. DR2). Melt inclusion and matrix glass compositions are dacitic and thus more evolved than the bulk rock composition (Table DR2). Here we focus on the concentrically zoned plagioclases, whereby melt inclusions were trapped along distinct mineral zones (Fig. 1; Fig. DR2). These melt inclusions likely formed as a result of rapid crystal growth, perhaps after a period of dissolution, and thus record a relative time series that reflects magma reservoir evolution (cf. Metrich and Wallace, 2008). Other crystals that display more complex textures (such as patchy zoning) were avoided, because it could not be guaranteed that these crystals grew progressively from core to rim.

The 2014 Kelud pumices are microlite poor (microlite number densities <200 mm⁻²; Fig. DR2). Microlites usually nucleate at high degrees of undercooling, for example during decompression upon ascent (Hammer and Rutherford, 2002). The general lack of microlites suggests that the 2014 magma ascended rapidly relative to the 2007 effusive eruption (>54200 mm⁻²), consistent with the high eruption intensity and eruptive plume in 2014 (Caudron et al., 2015). This is because microlites need tens of hours to grow in undercooled silicic systems (Hammer and Rutherford, 2002). The limited difference between melt inclusion and matrix glass chemical data for the 2014 pumice also demonstrates minimal crystal growth upon ascent (Table DR2). This evidence, coupled with the microlite-poor groundmass, suggests that melt inclusions in the 2014 phenocrysts were trapped within the magma reservoir rather than upon ascent.

A potential problem affecting melt inclusion H₂O contents is the diffusion of H⁺, as has been well demonstrated in the case of olivine-hosted melt inclusions in mafic magmas (Portnyagin et al., 2008; Gaetani et al., 2012). Experiments and models in these studies predict that diffusive H⁺

transfer will be greater for smaller host crystals, smaller melt inclusions, and inclusions closer to the crystal rim. To evaluate this potential effect, melt inclusion H₂O contents were tested against host crystal size, inclusion position, and size (Fig. DR3). No significant correlations exist between H₂O content and melt inclusion size, distance from the rim, or crystal size ($n = 51$, p values are >0.01; Fig. DR3). From these observations, we infer that H⁺ diffusion had no significant effect on the H₂O contents measured in the Kelud melt inclusions. The apparent absence of H⁺ diffusion may be attributed to minimal H₂O concentration gradients between inclusions and the host magma during crystal residence, coupled with fast magma ascent prior to and during the 2014 eruption, which would severely limit the time for diffusion under an H₂O gradient. During magma storage, the activity gradient between the melt inclusions and carrier melt was calculated at -0.07, which is comparable with values of ~0.04 that Hartley et al. (2015) argued may have been too small to facilitate H⁺ diffusion through olivine crystals. However, if diffusion occurred under these low activity gradients, calculated diffusive time scales range from 1 week to 5 months. Consequently, there may not be enough time for H⁺ to diffuse and water contents to equilibrate in a carrier melt with a rapidly fluctuating volatile content (see the Data Repository; Table DR3).

Chemical and H₂O Variations Within Plagioclase Crystals

Chemical traverses from core to rim are shown on backscattered SEM images in Figure 1. Anorthite contents vary throughout the crystals by up to 25 mol%, while minor elements in plagioclase (e.g., Fe) remain relatively constant. H₂O contents of small melt inclusions throughout the concentrically zoned feldspars range between 0.5 and 2.3 wt% (Fig. 1; Figs. DR4 and DR5; Table DR4) and vary systematically in accordance with the anorthite contents of the growth zones in which they are hosted. Specifically, low H₂O contents are observed in the higher anorthite zones while higher H₂O contents exist in the relatively low anorthite content zones. This same trend holds for the other concentrically zoned feldspars, as shown in Figure 2, and shows a significant negative correlation between the H₂O content of the melt inclusions and the anorthite content of the host plagioclase. A positive, albeit weak, correlation between H₂O and Cl provides further support that other volatile elements behave in a manner similar to that of H₂O (Fig. DR5). Given that an increased melt H₂O content stabilizes higher An plagioclase, and that these parameters should correlate positively (Putirka, 2005), the negative correlation shown in Figure 2 indicates that H₂O had a limited effect on equilibrium anorthite content in this instance.

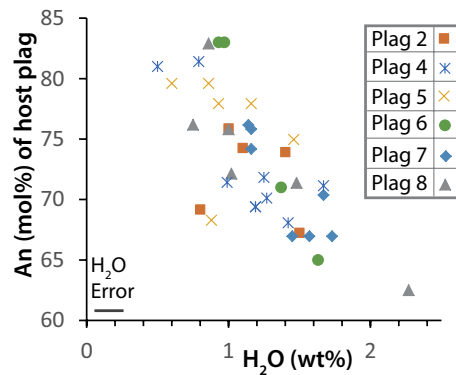


Figure 2. Plot of dissolved H₂O contents measured in the melt inclusions with Raman spectroscopy against anorthite content of the host plagioclase (plag) measured for six different crystals (Figs. DR4 and DR5; see footnote 1) (p value = 1.5×10^{-7} , $R^2 = 0.51$, $n = 41$). H₂O values measured via Fourier transform infrared spectroscopy on some melt inclusions confirm this range in H₂O contents (0.43–2.33 wt%; Table DR5).

As H₂O content does not seem to control anorthite values in Kelud 2014 plagioclases, and pressure is known to have a minimal impact on anorthite content (Blundy and Cashman, 2001), only a few possibilities to explain our observations remain. For example, Blundy et al. (2010) proposed that CO₂ fluxing can alter plagioclase and P_{H_2O} isothermally. However, CO₂ concentrations in the Kelud 2014 melt inclusions are low (<350 ppm) (Table DR5) and textures usually associated with CO₂-rich magmas, such as complex dissolution-reaction rims (Cashman and Blundy, 2013), are not observed here (Fig. DR2). Differences in crystal growth and cooling rates may also influence the H₂O content and anorthite relationship (Mollo et al., 2011). However, increases in Fe concentrations would then occur along with increasing anorthite, which is not recorded here (Fig. 1; Figs. DR4 and DR5). Using the proxy ratio of Cl/P₂O₅ in melt inclusions, significant effects from boundary layer entrapment can also be discounted (Baker, 2008) (Fig. DR3). Ruling out the factors described here points toward either a temperature control or an influx of compositionally different magma (e.g., mafic injections, in the case of reverse zoning). However, an influx of mafic magma would not only raise the anorthite content of plagioclase by adding more Ca to the system, but would also increase the concentrations of minor elements in plagioclase like Fe and Mg (Ruprecht and Wörner, 2007). In all of the EPMA traverses, measured minor elements remain fairly constant from core to rim, even when anorthite content changes considerably (Fig. 1; Figs. DR4 and DR5). Thus, if magma injections did occur, the evidence from major and minor elements is more consistent with the addition of compositionally similar magma. We therefore propose that

temperature is most likely the dominant factor controlling anorthite variability here.

Temperature changes are known to have large effects on anorthite content; for example, fluctuations of 50 °C changed the anorthite content by up to ~20 mol% in H₂O-saturated dacites from Mount St. Helens (Cashman and Blundy, 2013). To evaluate whether temperature changes can feasibly achieve the anorthite contents recorded at the specific measured H₂O contents in Kelud 2014 plagioclases, we employed the hygrometer of Waters and Lange (2015). Specifically, measured H₂O contents, along with plagioclase and liquid compositions (the latter from melt inclusion chemistry, where available) were modeled to solve for temperature (T). Figure 1 shows An-H₂O- T relationships and demonstrates that temperature fluctuations of up to 80 °C can explain the differences in anorthite content at the measured H₂O contents. After heating by magma injection, crystal growth likely occurred when magma started to cool again, thus the hottest temperatures may not have been recorded in the plagioclases.

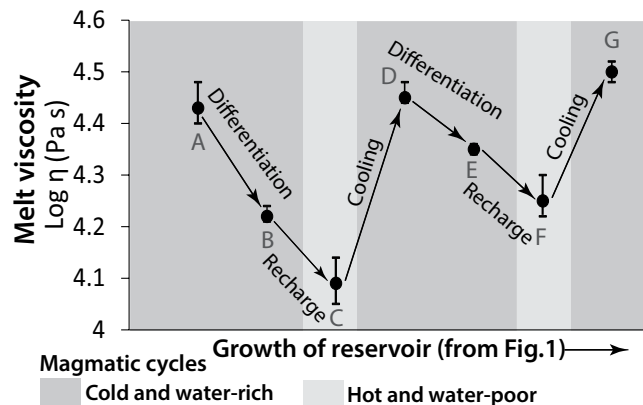
What Controls the Variation in Magma H₂O Contents?

Distinct temperature variations of up to 80 °C from plagioclase thermometry, coupled with the inference that zonal melt inclusions were formed by dissolution, implicates an additional heat source affecting the Kelud reservoir. Latent heat of crystallization may induce small temperature changes, but assuming latent heat release values similar to those of Blundy et al. (2006), these are likely to be considerably less than 80 °C. Heating could also occur from convective self-mixing with hotter parts of a zoned magma reservoir, or, perhaps more likely, from injections of hotter, but compositionally similar magma (Fig. DR6). If H₂O-undersaturated magma undergoes differentiation during cooling

periods, the dissolved H₂O content in the residual melt increases. Hotter, compositionally similar magma with lower H₂O content could then recharge the reservoir and thus dilute the total magma H₂O content.

The repeating hot and cold cycles that can occur within a magma reservoir (Fig. 1) not only affect volatile behavior and mineral chemistry, but also magma rheology as well as crystallization and mineral dissolution, which, in turn, affect magma ascent and eruption. Therefore, the point at which an eruption occurs within these hot and cold cycles may have a bearing on its explosivity. The eruptive style at Kelud volcano varies considerably. The last two eruptions illustrate this, with an effusive, dome-forming eruption in 2007 and an explosive Plinian eruption in 2014. Notably, all the plagioclase phenocrysts from the 2014 eruption examined in this study have low anorthite content rims. Because a minimal amount of ascent-driven crystallization is thought to have occurred prior to the 2014 eruption, the rim compositions (Fig. DR7) likely represent the final conditions within the magma reservoir immediately prior to the eruption. Thus, the magma reservoir prior to the 2014 eruption was in a relatively cold and H₂O-rich state and not directly associated with a magma recharge event. These conditions would lead to an increase in the available gas budget and magma viscosity, and so increase the likelihood of an explosive eruption (Fig. 3). The cooled state of the magma without recent magma recharge is consistent with the limited amount of precursory unrest recorded prior to the explosive 2014 eruption of Kelud (<2 weeks), which strongly contrasts with the higher estimated magma temperatures (1160 °C) and deep seismicity and high CO₂ emissions that were recorded up to four months prior to the 2007 effusive eruption (Caudron et al., 2012; Jeffery et al., 2013). In contrast, a magma recharge event likely preceded the 2007 eruption and lowered

Figure 3. Estimated melt viscosity values modeled for intensive fluctuations within the magma reservoir using the Giordano et al. (2008) model. The profile and letters A–G mimic the plagioclase traverse of Figure 1, using the values from measured H₂O contents, dacitic melt inclusion compositions, and calculated temperatures to calculate magma viscosity. The higher H₂O contents recorded during differentiation decrease magma viscosity, whereas temperature increases due to recharge events reduce melt viscosity to their lowest values. The error bars are the propagated errors of the model and H₂O content measurements. Bulk viscosity values (incorporating the measured 59% phenocryst content and 1.8 aspect ratio) would retain the rheological fluctuations observed, but would increase the viscosity by up to three orders (cf. Caricchi et al., 2007).



magma H₂O contents via volatile dilution, and likewise magma viscosity via an increase in temperature (Fig. 3) and decreased crystallinity (the 2007 magma had a phenocryst content ~6% lower than the 2014 magma). These combined factors may have favored an effusive eruption in 2007 as opposed to an explosive one, as seen in 2014. Volcanoes that are recharged by compositionally different and especially volatile-rich magmas present another variable to our proposed hot and cold cycles model, and can yield complex eruptive histories within individual volcanic systems.

CONCLUSIONS

Plagioclase anorthite melt inclusion H₂O systematics for the 2014 Kelud eruption record magma reservoir processes leading to large temperature fluctuations, which may have influenced magma rheology, degassing, and ultimately the eruptive style. Fine-scale measurements of melt inclusions at the crystal scale offer a promising new tool to decipher pre-eruptive assembly of magma reservoirs. Here we show that coupled thermal-H₂O cycles during the incremental growth of a magma reservoir at Kelud control eruptive style, where cooler, H₂O-rich periods dominated by differentiation favored explosive eruptions, and hotter, H₂O-poor periods following recharge by H₂O-poor magmas led to H₂O dilution, thus potentially favoring more effusive eruptions.

ACKNOWLEDGMENTS

This paper was helped by discussions with Laura Waters, as well as many scientists within the Memovolc (Measuring and Modelling Volcano Eruption Dynamics,) and the Volcanic and Magmatic Studies Group communities. Cassidy and Neave both acknowledge Humboldt fellowships. Field work was funded through the Swedish Research Council. We thank editor Brendan Murphy and three anonymous reviewers for their thorough and insightful comments.

REFERENCES CITED

Baker, D.R., 2008, The fidelity of melt inclusions as records of melt composition: *Contributions to Mineralogy and Petrology*, v. 156, p. 377–395, doi:10.1007/s00410-008-0291-3.

Behrens, H., Roux, J., Neuville, D.R., and Siemann, M., 2006, Quantification of dissolved H₂O in silicate glasses using confocal microRaman spectroscopy: *Chemical Geology*, v. 229, p. 96–112, doi:10.1016/j.chemgeo.2006.01.014.

Blundy, J., and Cashman, K., 2001, Ascent-driven crystallisation of dacite magmas at Mount St Helens, 1980–1986: *Contributions to Mineralogy and Petrology*, v. 140, p. 631–650, doi:10.1007/s004100000219.

Blundy, J., Cashman, K., and Humphreys, M., 2006, Magma heating by decompression-driven crystallization beneath andesite volcanoes: *Nature*, v. 443, p. 76–80, doi:10.1038/nature05100.

Blundy, J., Cashman, K.V., Rust, A., and Witham, F., 2010, A case for CO₂-rich arc magmas: *Earth*

and *Planetary Science Letters*, v. 290, p. 289–301, doi:10.1016/j.epsl.2009.12.013.

Burgisser, A., and Bergantz, G.W., 2011, A rapid mechanism to remobilize and homogenize highly crystalline magma bodies: *Nature*, v. 471, p. 212–215, doi:10.1038/nature09799.

Caricchi, L., Burlini, L., Ulmer, P., Gerya, T., Vassalli, M., and Papale, P., 2007, Non-Newtonian rheology of crystal-bearing magmas and implications for magma ascent dynamics: *Earth and Planetary Science Letters*, v. 264, p. 402–419, doi:10.1016/j.epsl.2007.09.032.

Cashman, K., and Blundy, J., 2013, Petrological cannibalism: The chemical and textural consequences of incremental magma body growth: *Contributions to Mineralogy and Petrology*, v. 166, p. 703–729, doi:10.1007/s00410-013-0895-0.

Caudron, C., Mazot, A., and Bernard, A., 2012, Carbon dioxide dynamics in Kelud volcanic lake: *Journal of Geophysical Research*, v. 117, B05102, doi:10.1029/2011JB008806.

Caudron, C., Taisne, B., Garces, M., Alexis, L.P., and Mialle, P., 2015, On the use of remote infrasound and seismic stations to constrain the eruptive sequence and intensity for the 2014 Kelud eruption: *Geophysical Research Letters*, v. 42, p. 6614–6621, doi:10.1002/2015GL064885.

Cooper, K.M., and Kent, A.J.R., 2014, Rapid remobilisation of magmatic crystals kept in cold storage: *Nature*, v. 506, p. 480–483, doi:10.1038/nature12991.

Gaetani, G.A., O'Leary, J.A., Shimizu, N., Bucholz, C.E., and Newville, M., 2012, Rapid reequilibration of H₂O and oxygen fugacity in olivine-hosted melt inclusions: *Geology*, v. 40, p. 915–918, doi:10.1130/G32992.1.

Giordano, D., Russell, J.K., and Dingwell, D.B., 2008, Viscosity of magmatic liquids: A model: *Earth and Planetary Science Letters*, v. 271, p. 123–134, doi:10.1016/j.epsl.2008.03.038.

Hammer, J.E., and Rutherford, M.J., 2002, An experimental study of the kinetics of decompression-induced crystallization in silicic melt: *Journal of Geophysical Research*, v. 107, p. ECV 8-1–ECV 8-24, doi:10.1029/2001JB000281.

Humphreys, M.C.S., Menand, T., Blundy, J.D., and Klimm, K., 2008, Magma ascent rates in explosive eruptions: Constraints from H₂O diffusion in melt inclusions: *Earth and Planetary Science Letters*, v. 270, p. 25–40, doi:10.1016/j.epsl.2008.02.041.

Hartley, M.E., Neave, D.A., MacLennan, J., Edmonds, M., and Thordarson, T., 2015, Diffusive over-hydration of olivine-hosted melt inclusions: *Earth and Planetary Science Letters*, v. 425, p. 168–178, doi:10.1016/j.epsl.2015.06.008.

Jeffery, A.J., et al., 2013, The pre-eruptive magma plumbing system of the 2007–2008 dome-forming eruption of Kelut volcano, East Java, Indonesia: *Contributions to Mineralogy and Petrology*, v. 166, p. 275–308, doi:10.1007/s00410-013-0875-4.

Kent, A.J.R., 2008, Melt inclusions in basaltic and related volcanic rocks, *in* Putirka, K.D., and Tepley, F.J., eds., *Minerals, inclusions and volcanic processes: Reviews in Mineralogy and Geochemistry*, v. 69, p. 273–331, doi:10.2138/rmg.2008.69.8.

Kristiansen, N.I., Prata, A.J., Stohl, A., and Carn, S.A., 2015, Stratospheric volcanic ash emissions from the 13 February 2014 Kelut eruption: *Geophysical Research Letters*, v. 42, p. 588–596, doi:10.1002/2014GL062307.

Lloyd, A.S., Plank, T., Ruprecht, P., Hauri, E.H., and Rose, W., 2013, Volatile loss from melt inclusions in pyroclasts of differing sizes: *Contributions to Mineralogy and Petrology*, v. 165, p. 129–153, doi:10.1007/s00410-012-0800-2.

Long, D.A., 1977, *Raman spectroscopy*: New York, McGraw-Hill, 292 p.

Menand, S., Annen, C., and de Saint Blanquat, M., 2015, Rates of magma transfer in the crust: Insights into magma reservoir recharge and pluton growth: *Geology*, v. 43, p. 199–202, doi:10.1130/G36224.1.

Metrich, N., and Wallace, P.J., 2008, Volatile abundances in basaltic magmas and their degassing paths tracked by melt inclusions, *in* Putirka, K.D., and Tepley, F.J., eds., *Minerals, inclusions and volcanic processes: Reviews in Mineralogy and Geochemistry*, v. 69, p. 363–402, doi:10.2138/rmg.2008.69.10.

Mollo, S., Putirka, K., Iezzi, G., Del Gaudio, P., and Scarlato, P., 2011, Plagioclase-melt (dis)equilibrium due to cooling dynamics: Implications for thermometry, barometry and hygrometry: *Lithos*, v. 125, p. 221–235, doi:10.1016/j.lithos.2011.02.008.

Portnyagin, M., Almeev, R., Matveev, S., and Holtz, F., 2008, Experimental evidence for rapid water exchange between melt inclusions in olivine and host magma: *Earth and Planetary Science Letters*, v. 272, p. 541–552, doi:10.1016/j.epsl.2008.05.020.

Putirka, K.A., 2005, Igneous thermometers and barometers based on plagioclase plus liquid equilibria: Tests of some existing models and new calibrations: *American Mineralogist*, v. 90, p. 336–346, doi:10.2138/am.2005.1449.

Ruprecht, P., and Bachmann, O., 2010, Pre-eruptive reheating during magma mixing at Quizapu volcano and the implications for the explosiveness of silicic arc volcanoes: *Geology*, v. 38, p. 919–922, doi:10.1130/G31110.1.

Ruprecht, P., and Wörner, G., 2007, Variable regimes in magma systems documented in plagioclase zoning patterns: El Misti stratovolcano and Andahu monogenetic cones: *Journal of Volcanology and Geothermal Research*, v. 165, p. 142–162, doi:10.1016/j.jvolgeores.2007.06.002.

Siebert, L., and Simkin, T., 2002, *Volcanoes of the world: An illustrated catalog of Holocene volcanoes and their eruptions*: Smithsonian Institution Global Volcanism Program, Digital Information Series GVP-3, http://volcano.si.edu/search_volcano.cfm.

Sparks, R.S.J., Sigurdsson, H., and Wilson, L., 1977, Magma mixing: A mechanism for triggering acid explosive eruptions: *Nature*, v. 267, p. 315–318, doi:10.1038/267315a0.

Wallace, P.J., 2005, Volatiles in subduction zone magmas: Concentrations and fluxes based on melt inclusion and volcanic gas data: *Journal of Volcanology and Geothermal Research*, v. 140, p. 217–240, doi:10.1016/j.jvolgeores.2004.07.023.

Waters, L.E., and Lange, R.A., 2015, An updated calibration of the plagioclase-liquid hygrometer-thermometer applicable to basalts through rhyolites: *American Mineralogist*, v. 100, p. 2172–2184, doi:10.2138/am-2015-5232.

Manuscript received 27 July 2016

Revised manuscript received 23 September 2016

Manuscript accepted 27 September 2016

Printed in USA